AD-A147 005 LONGER-SCALELENGTH PLASMA PERTURBATIONS BY AN INTENSE LASER BEAM(U) NAVAL RESEARCH LAB WASHINGTON DC J A STAMPER ET AL. 28 SEP 84 NRL-MR-5173 1/1

UNCLASSIFIED F/G 20/9 NL

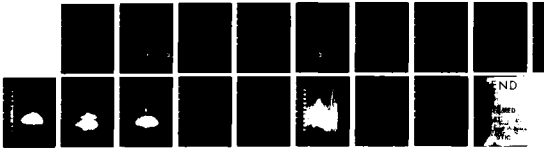

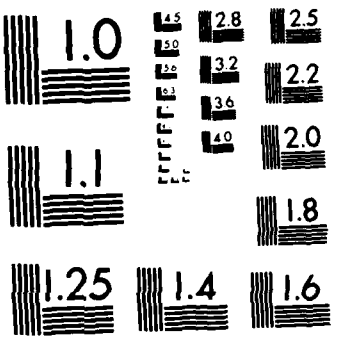

(2)

NRL Memorandum Report 5173

# Longer-Scalelength Plasma Perturbations by an Intense Laser Beam

J. A. STAMPER, F. C. YOUNG,* M. J. HERBST, S. P. OBENSCHAIN,
J. H. GARDNER,† R. H. LEHMBERG, E. A. MCLEAN,
J. GRUN, K. J. KEARNEY,‡ AND B. H. RIPIN

*Laser Plasma Branch*
*Plasma Physics Division*

**Plasma Technology Branch*
*Plasma Physics Division*

†*Laboratory for Computational Physics*

‡*Mission Research Corporation*
*Alexandria, VA 22312*



September 28, 1984

This work was supported by the U.S. Department of Energy.



NAVAL RESEARCH LABORATORY
Washington, D.C.

SECURITY CLASSIFICATION OF THIS PAGE

# REPORT DOCUMENTATION PAGE

| | |
|---|---|
| 1a REPORT SECURITY CLASSIFICATION<br>UNCLASSIFIED | 1b RESTRICTIVE MARKINGS |
| 2a SECURITY CLASSIFICATION AUTHORITY | 3 DISTRIBUTION/AVAILABILITY OF REPORT<br>Approved for public release; distribution unlimited. |
| 2b DECLASSIFICATION/DOWNGRADING SCHEDULE | |
| 4 PERFORMING ORGANIZATION REPORT NUMBER(S)<br>NRL Memorandum Report 5173 | 5 MONITORING ORGANIZATION REPORT NUMBER(S) |
| 6a NAME OF PERFORMING ORGANIZATION<br>Naval Research Laboratory<br>6b OFFICE SYMBOL (If applicable)<br>Code 4730 | 7a NAME OF MONITORING ORGANIZATION |
| 6c ADDRESS (City, State, and ZIP Code)<br>Washington, DC 20375-5000. | 7b ADDRESS (City, State, and ZIP Code) |
| 8a NAME OF FUNDING/SPONSORING ORGANIZATION<br>Department of Energy<br>8b OFFICE SYMBOL (If applicable) | 9 PROCUREMENT INSTRUMENT IDENTIFICATION NUMBER |
| 8c ADDRESS (City, State, and ZIP Code)<br>Washington, DC 20545 | 10 SOURCE OF FUNDING NUMBERS<br>PROGRAM ELEMENT NO. DOE<br>PROJECT NO. DE AI08-79-DP-40092<br>TASK NO.<br>WORK UNIT ACCESSION NO. 47-0859-0-4 |

11 TITLE (Include Security Classification)
Longer-Scalelength Plasma Perturbations by an Intense Laser Beam

12 PERSONAL AUTHOR(S) Stamper, J.A., Young, F.C., Herbst, M.J., Obenschain, S.P., Gardner, J.H., Lehmberg, R.H., McLean, E.A., Grun, J., Kearney, K.J.,* and Ripin, B.H.

| 13a TYPE OF REPORT | 13b TIME COVERED | 14 DATE OF REPORT (Year, Month, Day) | 15 PAGE COUNT |
|---|---|---|---|
| Interim | FROM _____ TO _____ | 1984 September 28 | 21 |

16 SUPPLEMENTARY NOTATION
*Mission Research Corporation, Alexandria, VA 22312
This work was supported by the U.S. Department of Energy.

| 17 COSATI CODES | | |
|---|---|---|
| FIELD | GROUP | SUB-GROUP |
| | | |
| | | |

18 SUBJECT TERMS (Continue on reverse if necessary and identify by block number)
Laser, Plasma, Long-scalelength, Self-focusing

19 ABSTRACT (Continue on reverse if necessary and identify by block number)

Plasmas with long (up to 400 microns at 0.1 critical density) density scalelengths are used in laser-plasma interaction experiments in order to more closely approximate the blowoff conditions expected for a high-gain ICF pellet. These long-scalelength plasmas are produced by focusing one beam (≈ 150 J, 4 nsec FWHM) of the Pharos II Nd laser ($\lambda$ = 1.054 micron) to a large focal spot (~ 1 mm). A second beam is tightly focused within this spot to produce intensities up to $10^{15}$ W/cm$^2$. The pulsewidth of the second beam is only 0.3 nsec to minimize hydrodynamic perturbation to the long-scalelength plasma. The peak intensities of the two beams occur at the same time. Plasma density perturbations are monitored by side-on imaging a second-harmonic emission. At low energy in the short-pulse beam, this emission occurs only at distances from the target surface corresponding to $n_c \leq n < n_c$, showing no evidence for perturbation of the long-scalelength low density plasma. However, at higher energy, emission is seen well in front of the target, in highly-localized, filamentary-appearing regions. This observation is consistent with the formation of a low density channel

(Continues)

| 20 DISTRIBUTION/AVAILABILITY OF ABSTRACT | 21 ABSTRACT SECURITY CLASSIFICATION |
|---|---|
| ☒ UNCLASSIFIED/UNLIMITED ☐ SAME AS RPT ☐ DTIC USERS | UNCLASSIFIED |
| 22a NAME OF RESPONSIBLE INDIVIDUAL<br>J. A. Stamper | 22b TELEPHONE (Include Area Code)<br>(202) 767-2683<br>22c OFFICE SYMBOL<br>Code 4732 |

DD FORM 1473, 84 MAR 83 APR edition may be used until exhausted
All other editions are obsolete

SECURITY CLASSIFICATION OF THIS PAGE

19. ABSTRACT (Continued)

along the high-intensity beam path. The tendency to form a channel is predicted by a 2-D hydrodynamics code. The structure, intensity dependence, and polarization of the second-harmonic emission are consistent with self-focusing. Self-focusing of the incident beam in this experiment is shown to be consistent with a steady-state, self-focusing theory.

CONTENTS


I. INTRODUCTION ..... 1

II. EXPERIMENTAL ARRANGEMENT ..... 2

III. RESULTS AND DISCUSSION ..... 3

IV. CONCLUSIONS ..... 6

ACKNOWLEDGMENTS ..... 7

REFERENCES ..... 16

# LONGER-SCALELENGTH PLASMA PERTURBATIONS BY AN INTENSE LASER BEAM

## I. INTRODUCTION

The object of this experiment is to study the interaction of a high-intensity laser beam with a long-scalelength plasma. The overall experiment has been described by M.J. Herbst.[1] Absorption and x-ray studies have also been documented.[2,3] Interest in longer-scalelength plasmas stems from conditions expected in the blowoff of an ICF reactor pellet. In the experiment, a long-pulse (4 nsec FWHM) beam is focused to a large (1 mm) focal spot to produce a plasma with a long density gradient scalelength. By varying the spot size of this beam, plasmas of three different scalelengths were reliably produced: long (400 μm at 0.1 $n_c$), medium (300 μm at 0.1 $n_c$), and short (200 μm at .1 $n_c$). A second, short-pulse (300 psec) is tightly focused (0.1 mm dia.) into the long scalelength plasma to produce a high intensity.

It was desired that the long scalelength plasma, which had been carefully characterized, not be greatly perturbed by the high intensity laser beam. To minimize these perturbations, the duration of the short pulse is only 300 psec (FWHM). Also, thermal conduction will help to smooth out some of the temperature variations in the plasma. Nevertheless, perturbations were seen. Measurements of x rays provided experimental evidence for additional heating during the short pulse.[3] Two-dimensional hydrodynamic calculations also showed additional heating of the plasma during the short pulse. In fact these calculations showed a density channel beginning to form along the path of the high-intense beam.[4] This report presents experimental evidence for density perturbations in the long-scalelength plasma and for self-focusing of

Manuscript approved July 12, 1984.

the high-intensity beam at incident energies above 15 J. This evidence is obtained from spatially-resolved, time-integrated images of second-harmonic emitted light which is observed when there is high energy in the short-pulse beam. Electrons, oscillating in response to the laser electromagnetic field, will produce (due to charge-separation effects) second-harmonic radiation when the oscillation is along a density gradient. Thus second-harmonic emission serves as a diagnostic of density structure.

## II. Experimental Arrangement

The experimental arrangement is illustrated in Fig. 1. As explained in the Introduction, the two beams of the NRL, Pharos II Nd-glass laser beam (1.054 μm) were focused onto planar polystyrene (CH) foil targets to produce a high intensity laser beam interacting with a long scalelength plasma. The longer-pulse (4 nsec FWHM), loosely-focused (~ 1 mm) beam produced the longer-scalelength plasma while the short-pulse (0.3 nsec FWHM), tightly-focused (~ 0.1 mm) beam was at sufficiently high vacuum intensity ($10^{14}$ to $10^{15}$ W/cm$^2$) to study ICF physics issues. Both beams were circularly polarized on entering the target chamber. The light emitted from the plasma, parallel to the target surface, was collected and collimated with an f/2.8, 10-cm focal length lens. This light was focused onto film with a 50 cm focal-length lens to produce a recorded magnification of 5. A narrow band pass (12 Å FWHM) interference filter was used to select the second harmonic (5270 Å) wavelength. On some shots, a polarizing (Wollaston) prism was used to angularly separate the two polarizations so that separate images could be recorded in the two polarizations of emitted light.

## III. Results and Discussion

Figure 2 shows the second-harmonic emitted light pattern observed with a lower incident energy (10.1 J) of the short-pulse beam. For this shot, there was 178 J on target in the long pulse beam and a long scalelength plasma (~ 400 micron at 0.1 critical density) was produced. The direction of laser propagation is indicated with an arrow and dimensions can be judged from the 200 micron rulings. For these lower intensities ($\lesssim 3 \times 10^{14}$ W/cm$^2$) in the short-pulse beam one can see a large region of faint emission corresponding to the diameter (~ 1 mm) of the long-pulse beam. This is primarily plasma continuum radiation in the band-pass of the filter. One can also see a somewhat faint region of emission with transverse dimensions (0.1 mm) of the order of the diameter of the high-intensity beam. This is primarily second harmonic emission (verified by filter substitution at nearby wavelength), and it occurs at distances from the target corresponding to the critical to quarter-critical region in different shots. There is no evidence in these lower intensity shots that the long-scalelength plasma has been appreciably perturbed.

The emitted light pattern is markedly different for higher vacuum intensities ($\gtrsim 3 \times 10^{14}$ W/cm$^2$) in the short-pulse beam. The observed pattern is shown in Fig. 3 for 36 J in the short-pulse beam and for the long-scalelength background plasma. There is an intense region of unpolarized second-harmonic emission near the target surface. This is the expected emission from the quarter-critical to critical region. However, there is also a filamentary appearing region of emission well out (~ 1 mm) in front of the target. The density of the background plasma in this region is only a few percent of critical.

Another example of the second harmonic emission observed at higher intensities in the short-pulse beam is shown in Fig. 4. For this shot, there was 22 J in the short-pulse and a long-scalelength background plasma. Three regions of emission can be seen well out in front of the target.

Emission well out in front of the target is, in fact, a common feature for higher energies ($\gtrsim$ 15 J) in the high-intensity beam. This front-side emission was primarily polarized orthogonal to the direction of the laser. The range of distances from the target at which this front-side emission was observed on different shots is shown in Fig. 5. The distances are plotted as a function of energy in the high-intensity beam. The figure is keyed to show which shots were for long-scalelength, medium-scalelength, and short-scalelength plasmas. Front-side emission was seen only on a very small fraction of the lower energy shots. Note that there is a correlation between the scalelength of the background plasma and the distance from the target at which emission is observed. Emission is observed at greater distances for longer scalelengths. The distances correspond to nearly fixed background plasma density ($\sim$ 0.05 critical) which suggests that this emission may be due to the same process for all three scalelengths.

The most likely process to produce this filamentary appearing, localized emission at higher intensities is self-focusing of the high-intensity beam. A simple model for second harmonic emission in a low density channel can account for observed features of this emission. The polarization-resolved data showed that the emission well out in front of the target was primarily polarized in the plane orthogonal to the direction of laser while the emission near the surface was unpolarized. The polarization of the emission far from the target is consistent with its production in a radial density channel, as illustrated in Fig. 6. The circularly polarized incident laser beam produces circular

motion of electrons in the plasma. However, only the component of this motion which is radial in the density channel will oscillate the electrons along a density gradient and thus produce second harmonic emission. For a horizontal slice through middle of the channel, this radial motion is horizontal so that the side-on collection lens is in the null of the dipole radiation pattern. However, for a vertical slice through the channel, the radial motion and electric field are vertical, and the collection lens is at the maximum of the dipole radiation pattern. This accounts for the observed vertical polarization of the side-on collected light at large distances from the target. In contrast, polarization of the $2\omega_o$ emission observed near the target surface is consistent with expectations for electron oscillations across an axial density gradient.

There is also experimental evidence for reduced emission from the central region of the channel, which is also predicted by the above model. The second of the front-side emission regions given in Fig. 4 is shown further enlarged in Fig. 7. The scale units in this figure correspond to only 20 μm. One can see intense emission localized to a channel of only 3 or 4 μm diameter. At one position along the emission region there is a darker central region. As explained above, reduced central emission is expected when looking radially across the center of the channel due to the horizontal polarization along this viewing direction.

Most of the intense emission at the second harmonic frequency probably occurs after the beam has self-focused to a small radius. However, in order to get to this condition, there must be a self-focusing tendency under conditions of the intially focused beam. Hot spots with transverse dimensions of a few tens of microns could occur in the incident beam and lead to filamentation. Furthermore, the short-pulse beam is itself focused to a

vacuum diameter of 100 μm, and since some of the shots show a single transverse region of emission, the beam may undergo whole-beam self-focusing. One may ask whether, under conditions of the experiment, there is a theoretical basis for expecting sufficient growth of transverse wavelengths of 10 to 100 microns. The results of a steady-state, small-amplitude theory of self-focusing are plotted in Fig. 8. The theory, by R.H. Lehmberg,[5] includes both ponderomotive and thermal self-focusing contributions. One can see that for a CH target at irradiances (I) in the mid $10^{13}$ W/cm$^2$ range (and at $n_c/4$), transverse wavelengths greater than about 20 microns have growth lengths of only 100 microns. The larger growth lengths for smaller transverse wavelengths are due to diffraction becoming important. The theoretical growth lengths vary as $nI^{-1/2}$ (ponderomotive) and as $n^{-3/2}I^{-1/2}$ (thermal). Thus, in this experiment, with an average irradiance of mid-$10^{14}$ W/cm$^2$ and with density scalelengths of a few hundred microns at tenth critical, one could get self-focusing in the underdense region.

## IV. Conclusions

The two beams of the NRL, Pharos II laser beam were used to study the interaction of a high-intensity laser beam with a long-scalelength plasma. The long-pulse beam was loosely focused to produce the long-scalelength plasma, and the short pulse beam was tightly focused into the long-scalelength plasma to produce the high intensity. Spatially-resolved emission at the second harmonic wavelength was observed side on to the target surface. For lower energy in the short-pulse beam, this emission was observed at distances from the target corresponding to densities in the range $n_c/4$ to $n_c$, and there was no indication of a perturbation of the underdense plasma. However, at higher energy in the short-pulse beam, the emission occurs ~ 1 mm in front of

the target at a density ~ 0.05 $n_c$ in highly-localized (radially) regions. This is consistent with the formation of a low-density channel. Such a tendency was predicted by the 2-D calculations.

The filamentary appearing, highly-localized emission which occurs in the higher energy short-pulse shots provides evidence for self-focusing. Further evidence for self-focusing is found in the observed polarization of the front-side emission, which is consistent with electron oscillations in a channel produced by self-focusing. The tendency for the incident, high-intensity beam to self-focus was shown to be consistent with a steady-state theory. However, the large intensity variations between the two beams and the low temperature of the background plasma in the experiment would enhance self-focusing over that which may occur in an ICF pellet. Nevertheless, such experiments may allow a controlled study of self-focusing in a long-scalelength plasma. A generalization of the 2-D codes would be required to analyze the self-focusing. Ray tracing would have to be included and, perhaps, diffraction effects, relativistic effects and magnetic fields.

Acknowledgments

The work was supported by the U.S. Department of Energy. We wish to acknowledge the technical assistance of N. Nocerino, E. Turbyfill, and B. Sands.

# SECOND-HARMONIC EMISSION PARALLEL TO TARGET

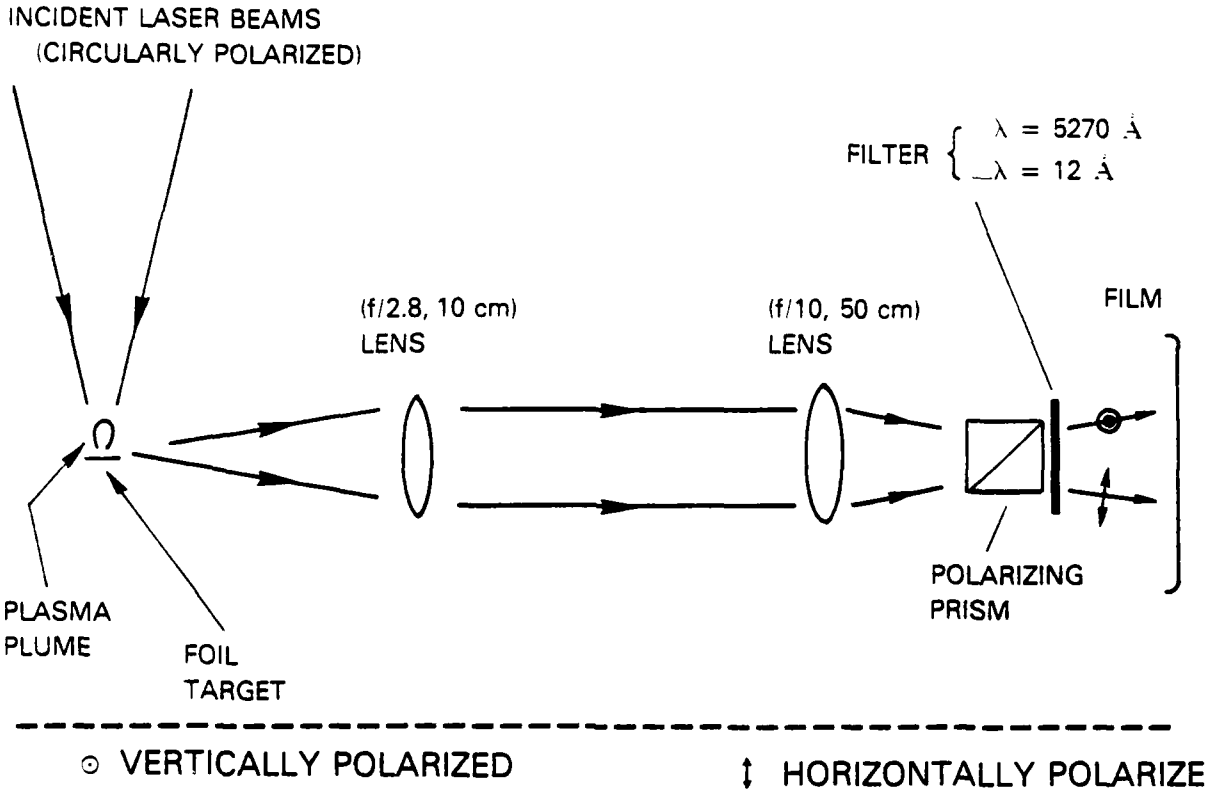


Figure 1 Experimental arrangement for making spatially-resolved, time-integrated observations of emission at the second-harmonic wavelength.

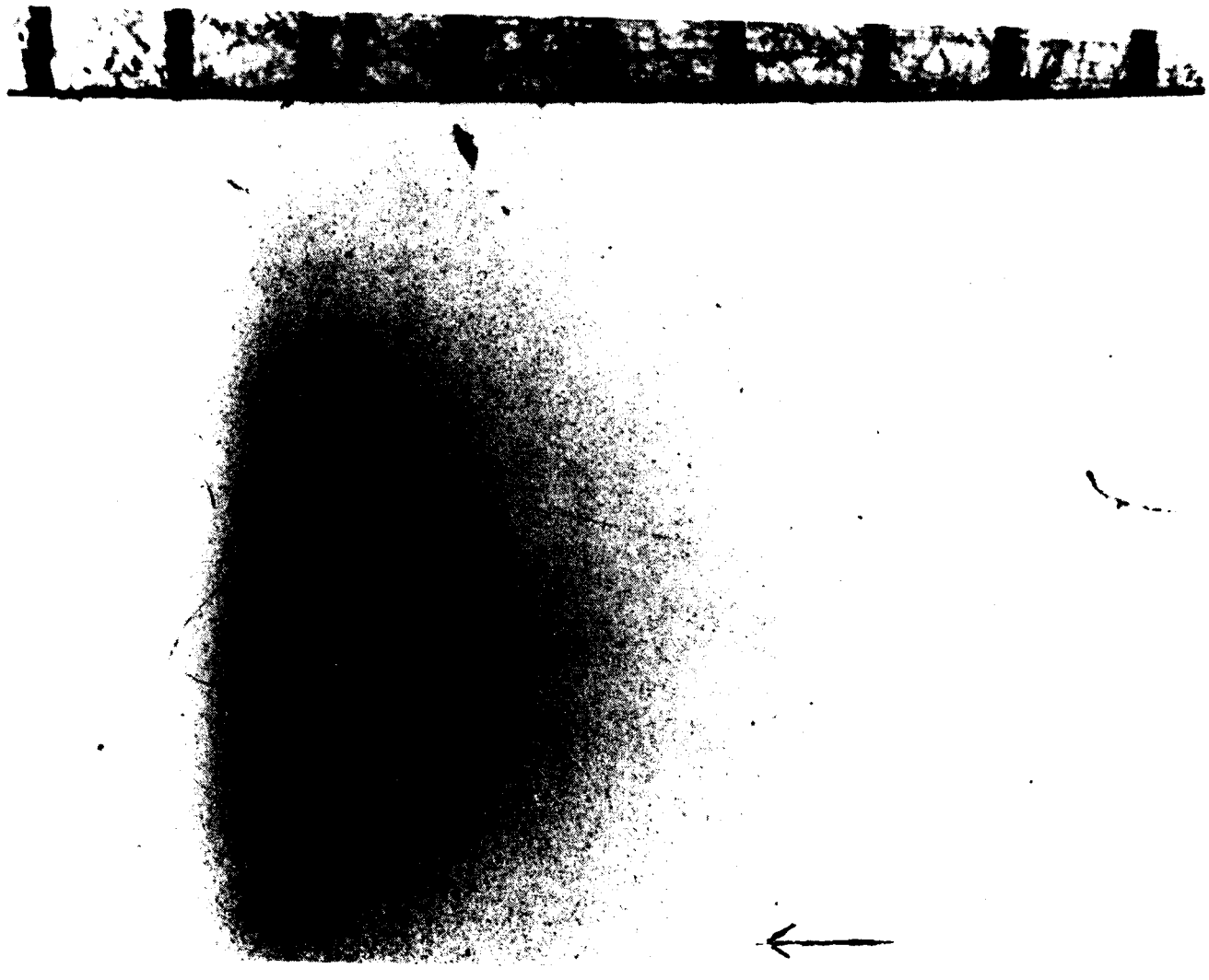

Figure 2 Typical emission pattern for low energy ($\lesssim$ 15 J) in the short-pulse beam. Note the large region of faint emission, corresponding to plasma continuum radiation in the band pass of the filter. A small region (0.1 mm diameter) of emission can also be seen on axis. This is primarily second-harmonic emission in the quarter-critical to critical region. 200 μm markers are provided.

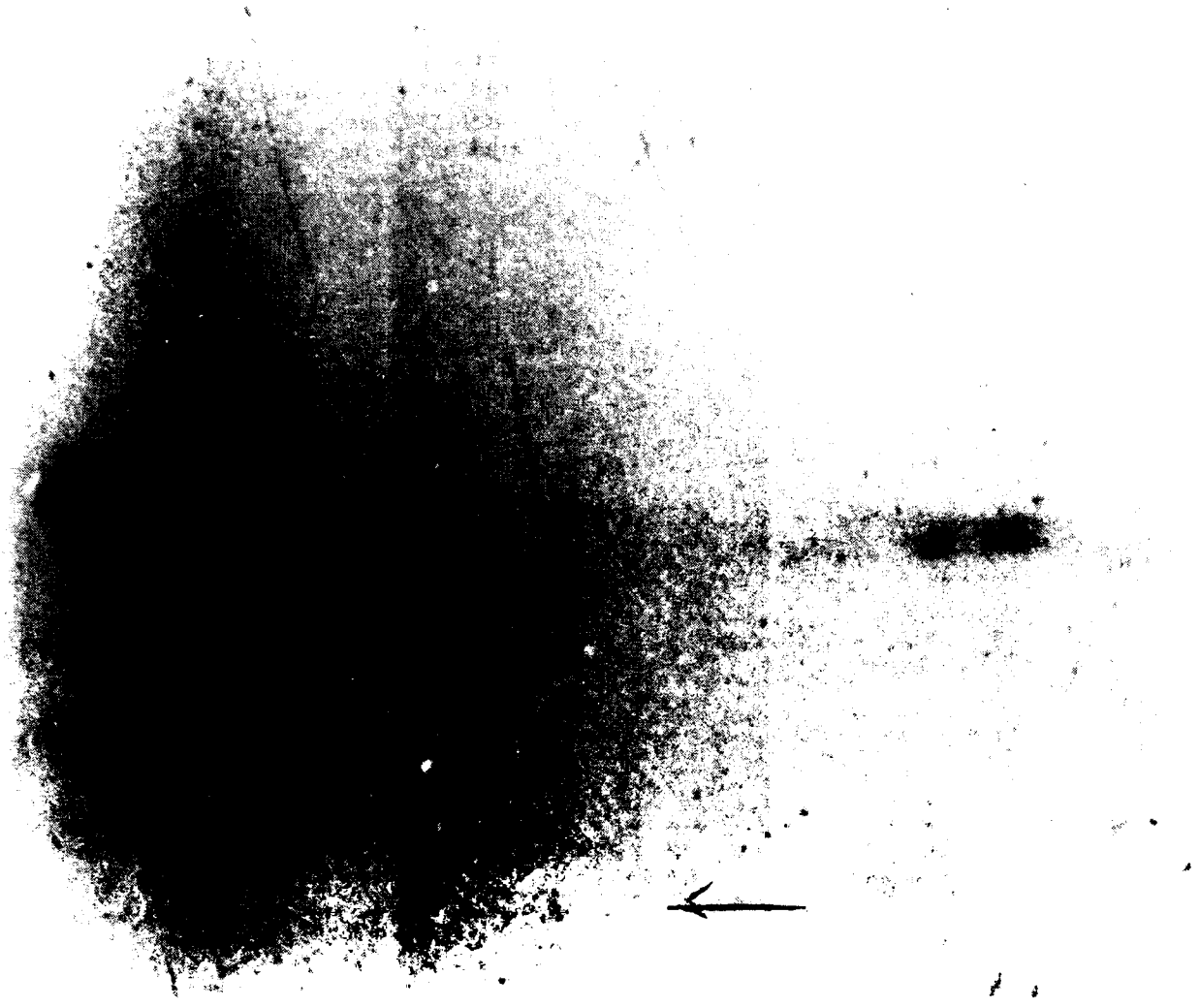

Figure 3 Emission pattern observed for high energy (36 J) in the short-pulse beam. In addition to an intense region of emission near the target surface, there is emission observed well out in the under-dense plasma, at about 1 mm from the target surface. Markers are 200 μm.

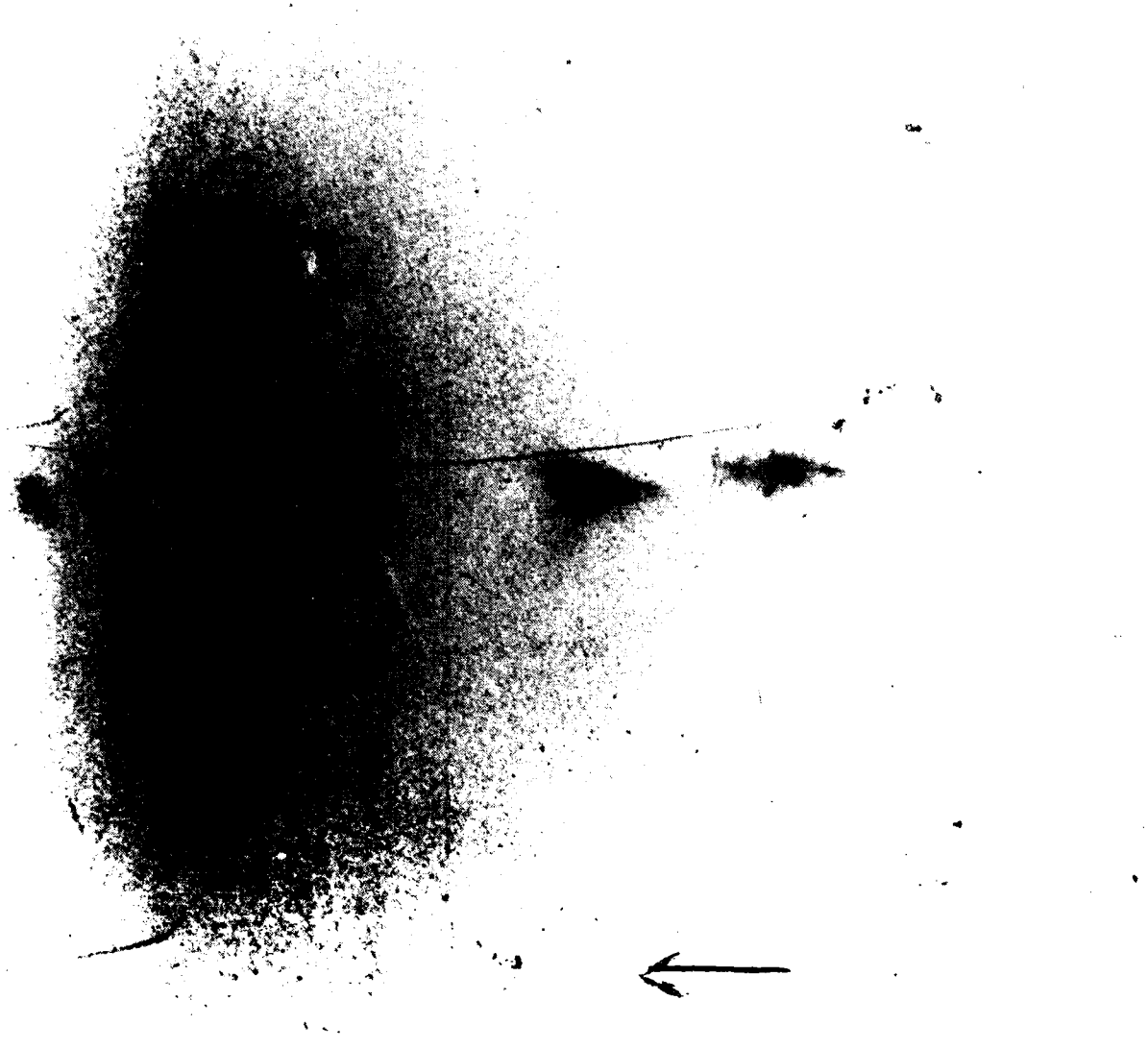

Figure 4 Emission pattern for a 22 J shot. Note the three regions of emission in the under-dense plasma. Markers are 200 μm.

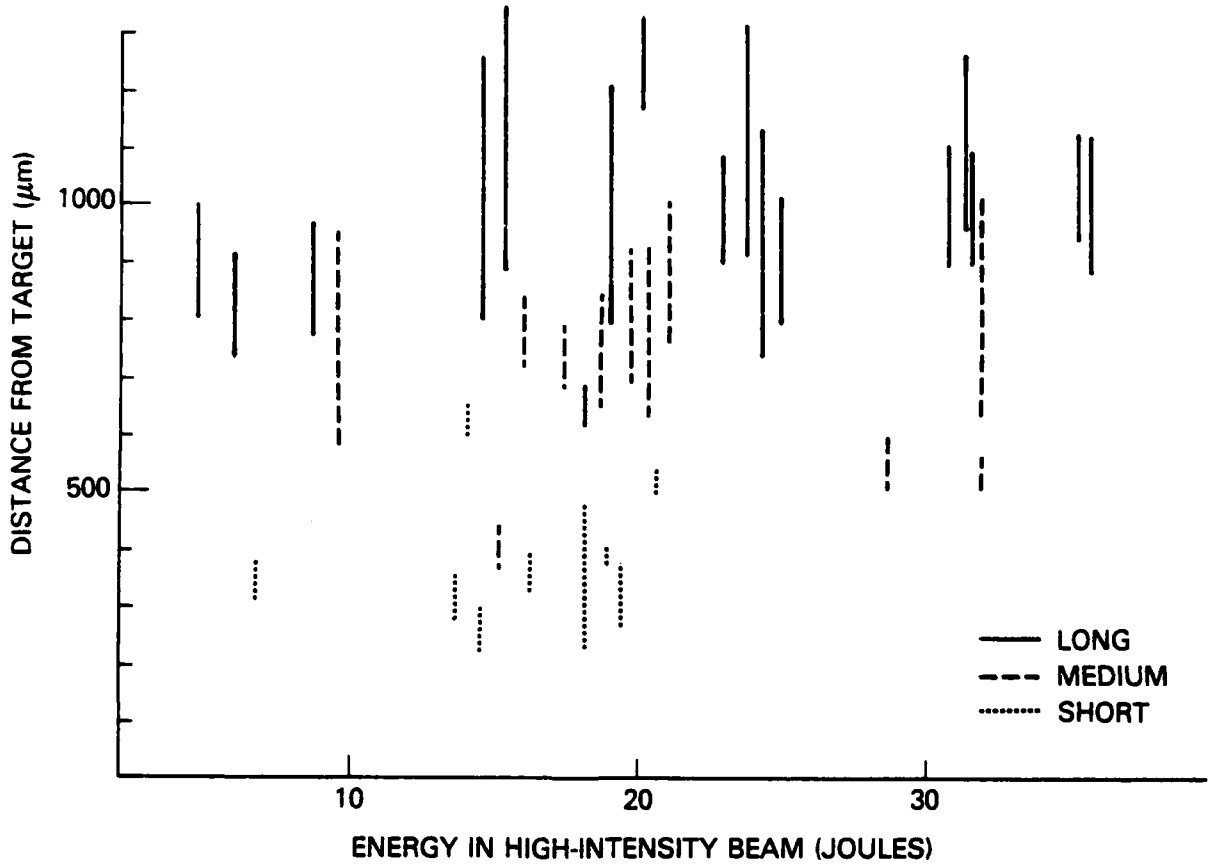


Figure 5 Range of distances from the target at which second-harmonic emission was observed as a function of energy in the high-intensity (short-pulse) beam. The plot is keyed to show which shots were for short-scalelength, medium-scalelength, and long-scalelength plasmas. Note that the emission is observed at greater distances for longer-scalelength plasmas.

# MODEL FOR HARMONIC EMISSION

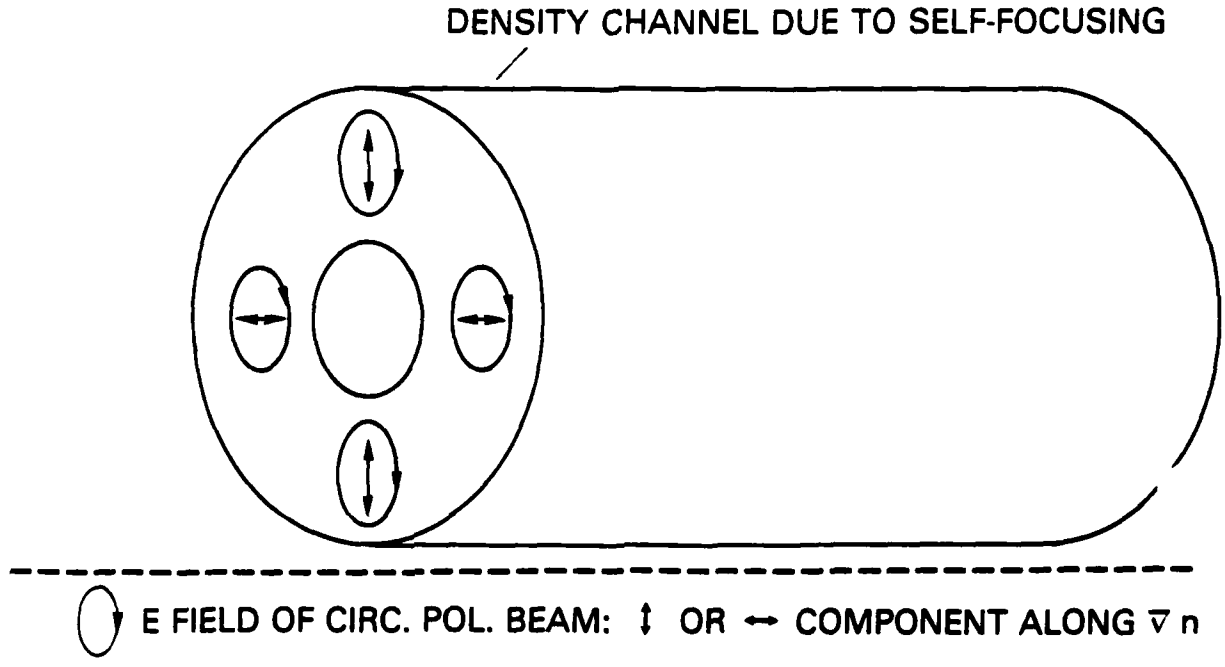


Figure 6 Illustration of model for explaining the observed polarization of second-harmonic emission from the low-density plasma. Only the radial component of the circular electron oscillations is along the density gradient and thus produce the emission.

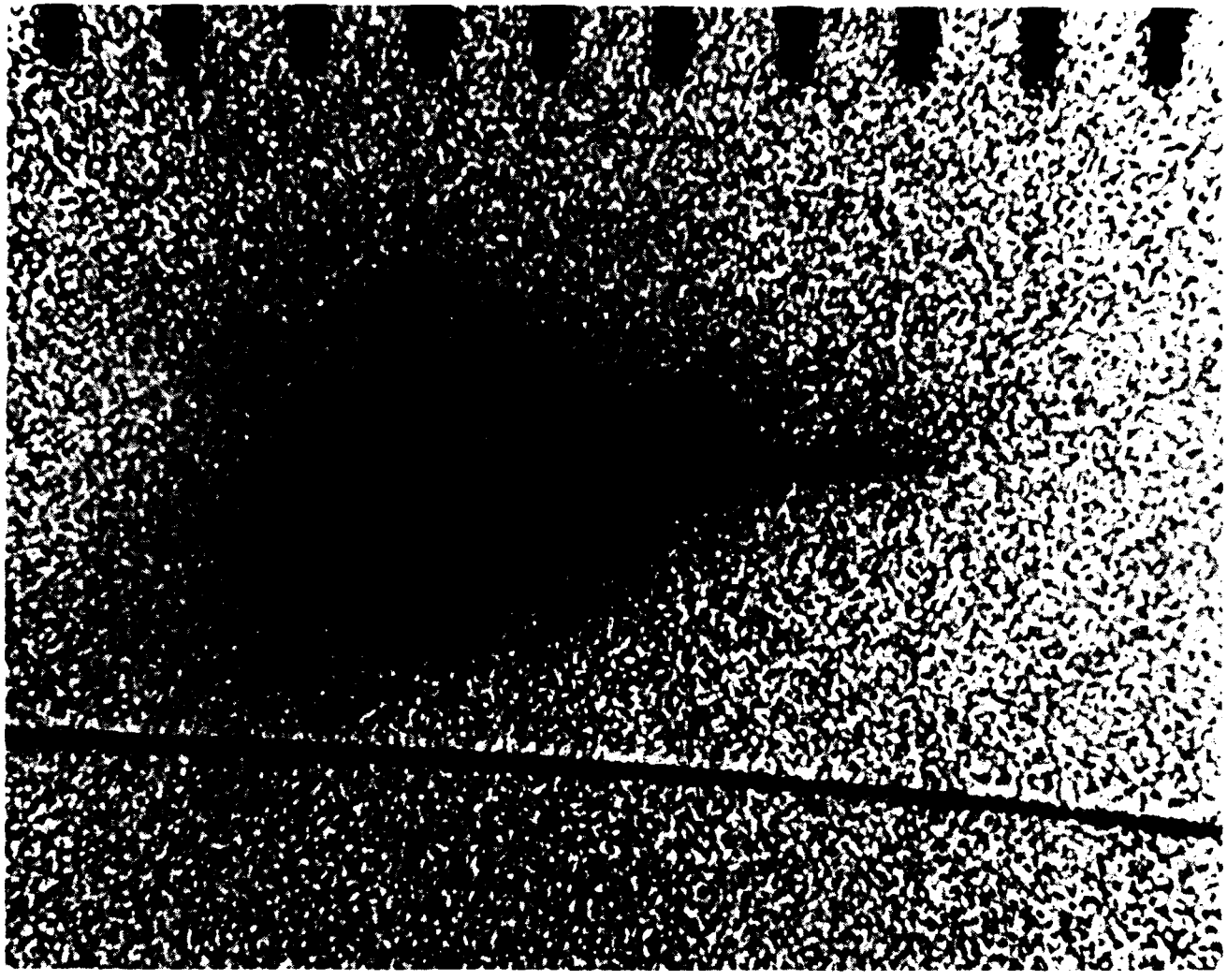

Figure 7 Highly-magnified view (markers are 20 μm) of the next-to-outer emission region shown in Fig. 4. Note that the radial extent of the intense emission is only a few microns and that a region of reduced emission can be seen on axis, at one location, with a diameter around one micron.

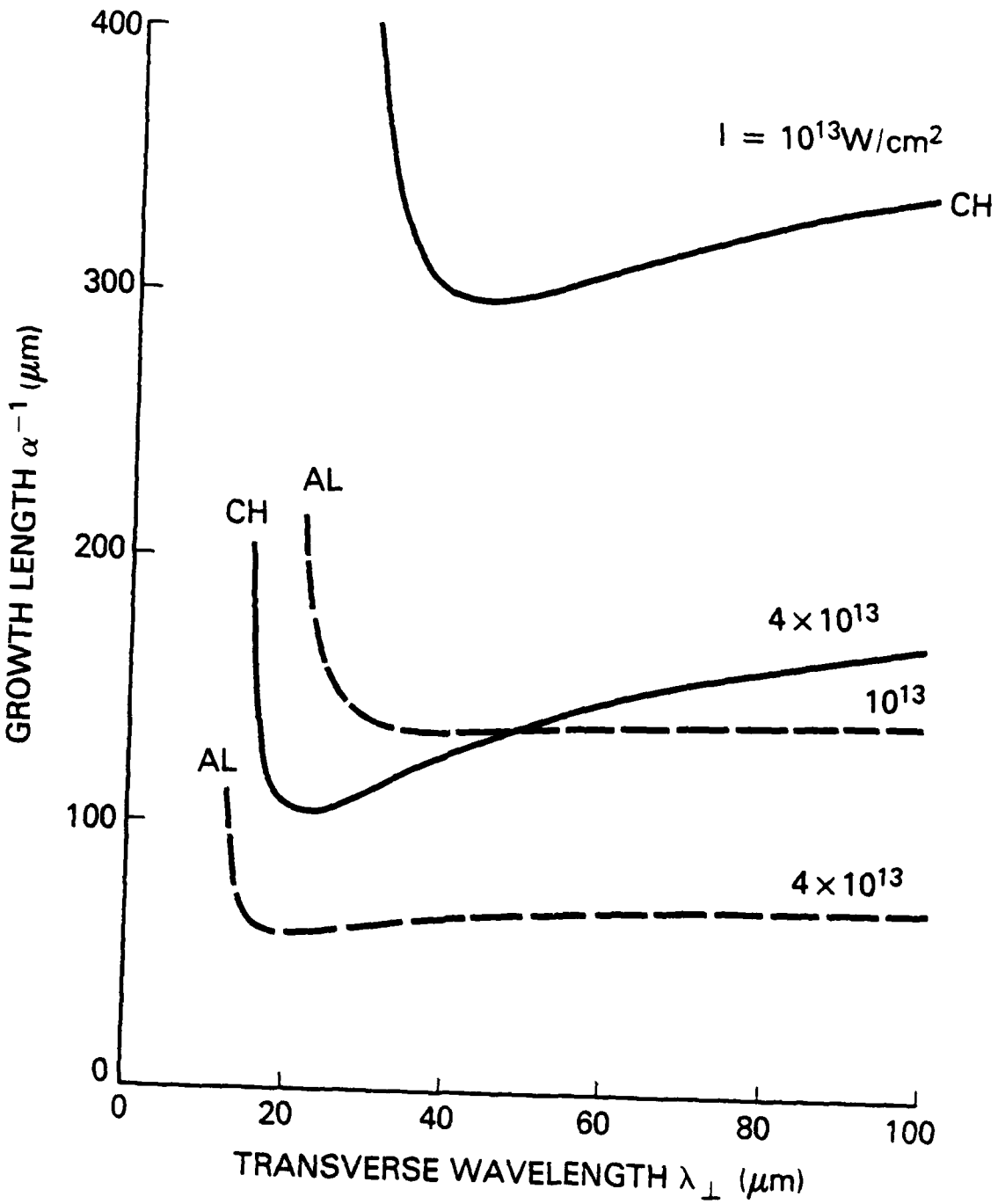


Figure 8 Theoretical variation of self-focusing growth length with transverse wavelength. The steady-state, small amplitude theory includes both ponderomotive and thermal self-focusing contributions.

References


1. M.J. Herbst, J. Grun, J. Gardner, J.A. Stamper, F.C. Young, S.P. Obenschain in the IAEA Proceedings of the Spring College on Radiation in Plasmas, International Centre for Theoretical Physics, Trieste (24 May-17 June 1983).

2. M.J. Herbst, J. Grun, J. Gardner, J.A. Stamper, F.C. Young, S.P. Obenschain, E.A. McLean, B.H. Ripin in Naval Research Laboratory Report No. 5186 (to be published, 1983). (AD-A134 759)

3. F.C. Young, M.J. Herbst, J.H. Gardner, K.J. Kearney, J.A. Stamper, S.P. Obenschain, J. Grun, E.A. McLean and B.H. Ripin in Naval Research Laboratory Report No. 5174 (unpublished, 1983). "X-Ray Production in Long-Scalelength Laser-Plasma Interaction Experiments."

4. J.H. Gardner, M.H. Emery, J. Grun, M.J. Herbst, R.L. Lehmberg, E.A. McLean, J.A. Stamper, F.C. Young, presented at the 13th Annual Anomalous Absorption Conference, Alberta, Canada, June 5-10, 1983.

5. R.H. Lehmberg in Section IIIC of Naval Research Laboratory Memorandum Report No. 4983 (unpublished, 1982) by M.J. Herbst, J.A. Stamper, R.H. Lehmberg, R.R. Whitlock, F.C. Young, J. Grun, and B.H. Ripin. (AD-A123 643)

END

FILMED

11-84

DTIC